

An Iterative Quantum Approach for Transformation Estimation from Point Sets

Appendix

This supplementary material adds mathematical detail to the main paper and contains further information regarding the computations on D-Wave. More precisely, we provide

- fully explicit formulae for the linearized rotation matrices in 2D and 3D (Appendix A.1),
- a derivation of the objective function that appears in the QUBO problem (Appendix A.2),
- visualizations of the embedding of the QUBO problems in the D-Wave 2000Q QPU and of the histograms of the sampled energies (Appendix B).

A. Derivations

A.1. Linearization of Rotation Matrices

We aim to provide detailed formulae for the terms R_c and R_i appearing in the main paper in Eq. (13), resp., Eq. (19):

$$R\tilde{y}_i \approx R_c\tilde{y}_i + R_i\hat{v}. \quad (27)$$

The 2D case. We recall from Eq. (12) and Eq. (14) that in the 2D case we have

$$R_c = \left[g(\theta_c) - g'(\theta_c)\Delta \right] I + \left[h(\theta_c) - h'(\theta_c)\Delta \right] S \quad (28)$$

and

$$R_i = \left[g'(\theta_c)I + h'(\theta_c)S \right] \tilde{y}_i, \quad (29)$$

where $g(t) = \cos t$, $g'(t) = -\sin t$, $h(t) = \sin t$ and $h'(t) = \cos t$, and S is defined in Eq. (9).

The 3D case. Inserting $v = v_c - \Delta + \hat{v}$ into Eq. (17) yields

$$\begin{aligned} R(\hat{v}) \approx & I + \left[g(v_c) + g'(v_c)(\hat{v} - \Delta) \right] M_c + g(v_c)M(\hat{v} - \Delta) \\ & + \left[h(v_c) + h'(v_c)(\hat{v} - \Delta) \right] M_c^2 \\ & + h(v_c) \left[M(\hat{v} - \Delta)M_c + M_cM(\hat{v} - \Delta) \right], \end{aligned} \quad (30)$$

where $M_c := M(v_c)$, $g(v) = (\sin \|v\|_2) / \|v\|_2$, $h(v) = (1 - \cos \|v\|_2) / \|v\|_2^2$,

$$\begin{aligned} g'(v) &= v^\top \cdot \left(\frac{\|v\|_2 \cos \|v\|_2 - \sin \|v\|_2}{\|v\|_2^3} \right) \quad \text{and} \\ h'(v) &= v^\top \cdot \left(\frac{\|v\|_2 \sin \|v\|_2 - 2(1 - \cos \|v\|_2)}{\|v\|_2^4} \right). \end{aligned} \quad (31)$$

Using the linearity of $M(\cdot)$, cf. the definition of M in Eq. (15), we can rearrange this as

$$\begin{aligned} R(\hat{v}) \approx & I + \left[g(v_c) - g'(v_c)\Delta \right] M_c - g(v_c)M(\Delta) \\ & + \left[h(v_c) - h'(v_c)\Delta \right] M_c^2 \\ & - h(v_c) \left[M(\Delta)M_c + M_cM(\Delta) \right] \\ & + \left[g(v_c) + h(v_c)M_c \right] M(\hat{v}) \\ & + h(v_c)M(\hat{v})M_c + M_c g'(v_c)\hat{v} + M_c^2 h'(v_c)\hat{v}. \end{aligned} \quad (32)$$

The first three lines on the right-hand side of this expression define R_c (cf. Eq. (18)). As detailed in the paper, multiplying the last two lines on the right-hand side of this expression by \tilde{y}_i implies, after some manipulation, that

$$\begin{aligned} R_i &= M_c\tilde{y}_i g'(v_c) + M_c^2\tilde{y}_i h'(v_c) \\ & - h(v_c)M(M_c\tilde{y}_i) - \left[g(v_c) + h(v_c)M_c \right] M(\tilde{y}_i), \end{aligned} \quad (33)$$

cf. Eq. (20). Thus, we have provided fully explicit representations for R_c and R_i .

A.2. Derivation of the Objective Function of the QUBO Problem

To derive the objective function of the QUBO problem we use Eq. (27) to linearize inside the Euclidean distance in (RPR), i.e.,

$$\begin{aligned} \|\tilde{x}_i - R\tilde{y}_i\|^2 &\approx \|\tilde{x}_i - R_c\tilde{y}_i - R_i\hat{v}\|^2 \\ &= \langle \tilde{x}_i, \tilde{x}_i \rangle - 2 \langle \tilde{x}_i, R_c\tilde{y}_i + R_i\hat{v} \rangle \\ &\quad + \langle R_c\tilde{y}_i + R_i\hat{v}, R_c\tilde{y}_i + R_i\hat{v} \rangle \\ &= \langle \tilde{x}_i, \tilde{x}_i \rangle - 2 \langle \tilde{x}_i, R_c\tilde{y}_i \rangle + \langle R_c\tilde{y}_i, R_c\tilde{y}_i \rangle \\ &\quad + 2 \langle R_c\tilde{y}_i - \tilde{x}_i, R_i\hat{v} \rangle + \langle R_i\hat{v}, R_i\hat{v} \rangle, \end{aligned} \quad (34)$$

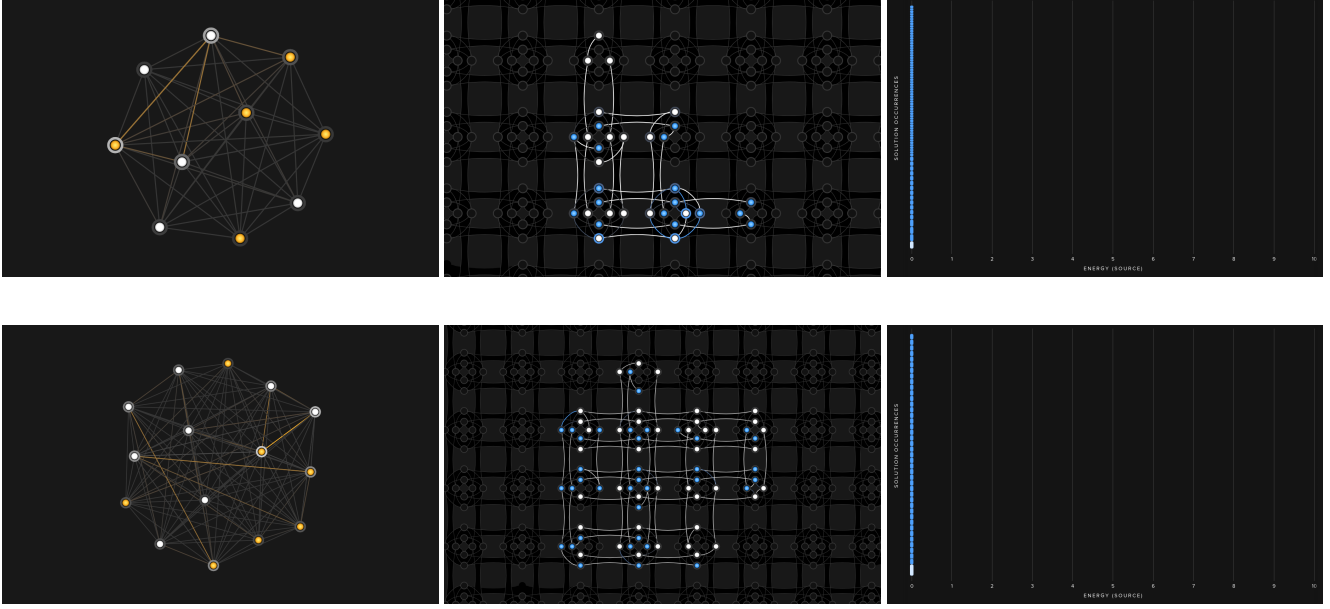


Figure 4. D-Wave problem inspections of the 2D (**first row**) and 3D (**second row**) TE problems after the 15th iteration of IQT. Shown are the connections between logical qubits (10 qubits in 2D and 15 qubits in 3D) as a connected graph (**first column**), the minor-embedding of the QUBOs into the chimera-graph topology of the D-Wave 2000Q’s QPU (**second column**) and the histograms of the sampled energies (**third column**). Note how the energies are concentrated on the left, indicating that the QPU samples good approximate solutions.

where R_c and R_i are as detailed in Appendix A.1. Recalling from Eq. (21) that $\hat{v} = Uq$ we obtain that, up to a constant that is independent of q ,

$$\|\tilde{x}_i - R\tilde{y}_i\|^2 \approx 2 \langle R_c \tilde{y}_i - \tilde{x}_i, R_i Uq \rangle + \langle R_i Uq, R_i Uq \rangle. \quad (35)$$

Summing over $i = 1, \dots, N$ this yields for the objective function $\sum_{i=1}^N \|\tilde{x}_i - R\tilde{y}_i\|^2$ in (RPR) the approximation

$$\sum_{i=1}^N 2(R_c \tilde{y}_i - \tilde{x}_i)^\top R_i Uq + \sum_{i=1}^N q^\top U^\top R_i^\top R_i Uq, \quad (36)$$

resulting in the QUBO problem

$$\min_{q \in \{0,1\}^{K_P}} q^\top Wq + c^\top q, \quad (37)$$

as stated in (QUBO) in the main paper, where

$$W = U^\top \left(\sum_{i=1}^N R_i^\top R_i \right) U \quad \text{and} \quad (38)$$

$$c = 2U^\top \sum_{i=1}^N R_i^\top (R_c \tilde{y}_i - \tilde{x}_i).$$

The parameter W and c can directly be passed to the D-Wave annealer to solve the problem on the hardware.

B. D-Wave Problem Inspection

In practice, embedding takes more physical than logical qubits because of the sparsity of connections between the physical qubits on currently available QPU chips. In order to create non-existing connections, the QPU *chains* a set of qubits by setting the strength of their connecting couplers negative enough to strongly correlate them [1]. Physical qubits in a chain correspond to the same logical qubit. In case of a chain breakage, the state of the qubit is determined by a majority vote of the qubits in the chain.

Fig. 4 presents the minor-embedding of the QUBOs for the 2D and 3D TE problems into the chimera topology of D-Wave 2000Q. The images are obtained from the D-Wave Leap problem inspector. We also display the histograms of the sampled energies in both cases. Note how the minimal energy solutions found by the QPU are all close to zero. This indicates that the solutions found by the QPU are very close to each other (which is not surprising since they are all expected to be close to the optimal solution).

References

- [1] D-Wave Systems. QPU Solver Datasheet. https://docs.dwavesys.com/docs/latest/doc_qpu.html, Oct 2021. 2